Perspective

Zeolite-Based Electrolytes: A Promising Choice for Solid-State Batteries

Malin Li,[1,2] Xiwen Chi,[1,2] and Jihong Yu[1,2,*]

[1] *State Key Laboratory of Inorganic Synthesis and Preparative Chemistry, College of Chemistry, Jilin University, Changchun 130012, People's Republic of China*
[2] *International Center of Future Science, Jilin University, Changchun 130012, People's Republic of China*

(Received 16 August 2022; revised 22 November 2022; published 21 December 2022)

The large-scale application of intermittent renewable energy has boosted the prosperous development of secondary batteries for the past several decades. In comparison with batteries based on liquid electrolytes, solid-state batteries are regarded as the goal for future energy storage due to their superior safety, nonvolatilization, excellent mechanical strength, and high energy density. While conventional solid electrolytes (SEs) struggle with their intrinsic limitations, zeolites are emerging as a promising choice for the future SEs of solid-state batteries. Herein, first, we analyze the challenges faced by conventional SEs to highlight the significance of leveraging zeolite-based SEs in secondary batteries. Then, we discuss the application of zeolites in liquid and solid electrolytes and showcase the functions of zeolites contributing to the enhanced wettability, thermal stability, mechanical strength, electrochemical stability, and ionic conductivity of separators and/or SEs. Finally, we provide a perspective on the development directions for zeolite-based SEs toward the design of materials, extension of battery systems, investigation of the conductive mechanism, and their practical applications.

DOI: 10.1103/PRXEnergy.1.031001

I. INTRODUCTION

Secondary batteries are regarded as key to the storage and transportation of intermittent renewable energy [1–5]. Despite great progress in the past several decades, conventional secondary batteries based on liquid electrolytes still suffer from some problems, including the severe safety issue of flammable organic liquid electrolytes [6,7], insufficient practical energy density of batteries considering peripheral components [8–10], leakage and volatilization of liquid electrolytes [11], and the inferior stability and compatibility of liquid electrolytes against metal anodes [12] [Figs. 1(a) and 1(b)]. Replacing liquid electrolytes with solid electrolytes (SEs) has emerged as a promising strategy to solve these problems.

In general, SEs can be divided into three classes: organic SEs (or polymer SEs), inorganic SEs, and composite SEs. Organic SEs—consisting of metal salts and solid polymer hosts, such as polyethylene oxide (PEO), polyacrylonitrile (PAN), polymethyl methacrylate (PMMA), and poly(vinylidene fluoride) (PVDF)—display high flexibility and are light weight [Fig. 1(c)] [13]. It is worth noting that ignitable polymer hosts (e.g., PEO, PAN, and PMMA) may challenge the safety of batteries, and thus, initial research efforts were devoted to the development of fireproof polymer composite electrolytes [14,15]. In addition, the intrinsic softness of organic SEs is disadvantageous for suppressing dendrite growth on metal anodes, although it ensures good physical contact between electrolytes and electrodes [16]. By contrast, nonflammable inorganic SEs are widely accepted to prevent the thermal runaway of batteries, and their superior mechanical strength is conducive for alleviating the dendrite-growth issue [Fig. 1(d)] [17]. Generally, inorganic SEs mainly comprise the oxides represented by garnet-type [18–21], perovskite-type [22–25], and sodium superionic conductor (NASICON) type [26–32] materials; the sulfides typified by Li_2S-P_2S_5 [33–36] and Li_2S-GeS_2-P_2S_5 [37–39]; as well as other types of SEs including hydrides and halides. As a hybrid material, the composite SE combines the merits of both inorganic and polymer SEs, achieving enhanced bulk and interfacial ionic conduction compared with polymer and inorganic SEs, respectively. Nonetheless, achieving a uniform composition of organic and inorganic components is challenging, and the stability of composite SEs is still unsatisfactory. In summary, all types of conventional SEs present specific limitations for practical applications, which leave room for the development of new SEs.

---

[*] jihong@jlu.edu.cn

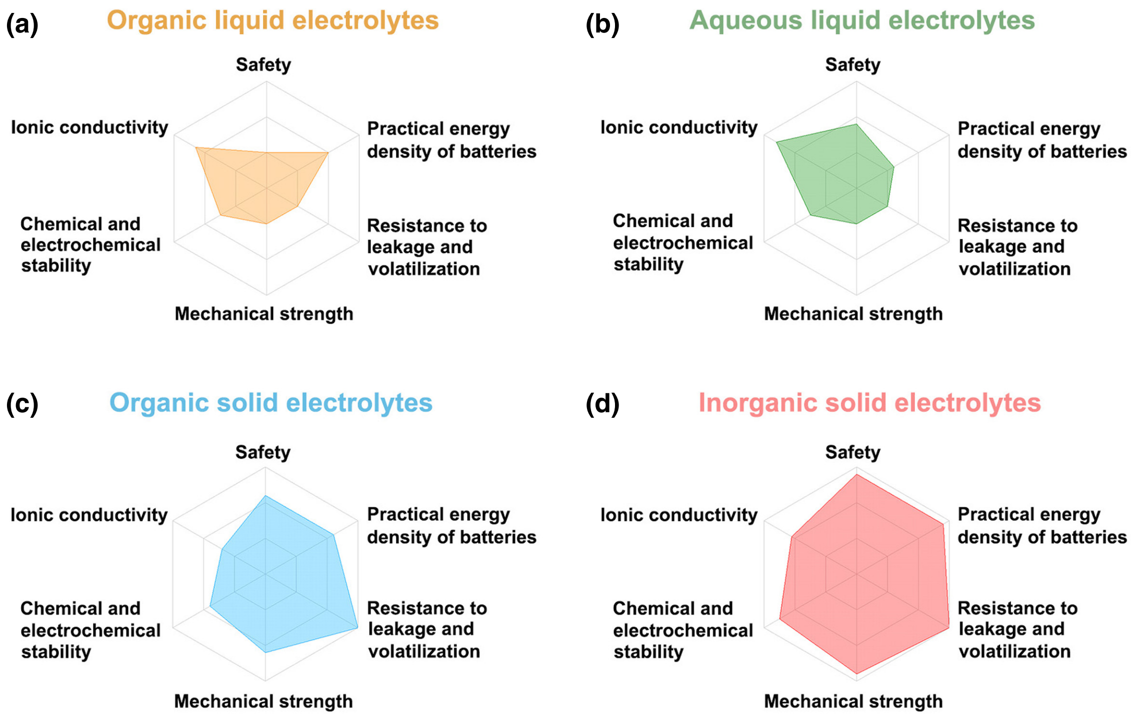

FIG. 1. Performance of liquid and solid electrolytes. Radar plots of the properties of organic liquid electrolytes (a), aqueous liquid electrolytes (b), organic solid electrolytes (c), and inorganic solid electrolytes (d).

Zeolites are a class of inorganic crystalline material constructed from corner-sharing TO_4 tetrahedra ($T =$ Si, Al, P, etc.) with ordered microporous structures [40]. On account of the superior (hydro)thermal stability, unique porous framework, and tunable acid active sites, zeolites are widely applied in many industrial fields, such as catalysis, separation, adsorption, and ion exchange [41–43]. As for application in secondary batteries, zeolites are employed as functional layers on separators or electrodes and additives of composite SEs in the early stage [44–46], while the application potential of zeolites in ion transport is not adequately recognized. Recently, our group reported LiX zeolite membrane as the solid electrolyte [47], addressing the bottleneck of conventional SEs for Li-air batteries. With superior properties, zeolite-based electrolytes exhibit great potential for various energy storage devices, although they are still in their infancy. Here, we discuss the salient features of zeolites as a new type of SE, evolution of the application of zeolites in secondary batteries, and future development directions for zeolite-based electrolytes.

II. REASONS FOR CHOOSING ZEOLITES

Conventional SEs inevitably encounter some problems in practical applications, including insufficient chemical and electrochemical stability, unsatisfactory ion transport, and interior dendrite formation, while zeolites present salient advantages to solve these problems. To gain a better understanding of the advantages of zeolites, Table I provides a specific comparison between the representative LiX zeolite and typical conventional SEs for lithium batteries.

A. Chemical and electrochemical stability

In general, decomposition occurs in some common SEs under the attack of water vapor and carbon dioxide, resulting in degradation of the crystal structure and a decrease in ionic conductivity. For example, sulfide SEs, with state-of-the-art ion conductivity among SEs, tend to be hydrolyzed in air accompanied by the release of H_2S [55]. Although the oxide SEs are generally more stable than sulfide SEs, typical garnet-type $Li_7La_3Zr_2O_{12}$ (LLZO) [50,51] and perovskite-type $Li_2SrTa_2O_7$ [17] still react with H_2O and CO_2. It is proven that the stability of SEs can be improved via composition tuning, additive mixing, and element doping [56–58], but the instability problems cannot be solved fundamentally, and the ionic conduction of SEs may be affected to some extent. By contrast, zeolites possess high intrinsic stability against ambient air [47,59], which is advantageous, considering the cost of processing, transportation, and storage or the requirement for open systems as metal-air batteries.

In addition, (electro)chemical reactions involving the generation of a new phase may occur at the interface of conventional SEs and electrodes. For instance, typical SEs with high-valence elements, including Ti-containing

TABLE I. Specific comparison between zeolite-based SEs and several typical SEs.

Type and material	Ionic conductivity ($S\,cm^{-1}$)	Electronic conductivity ($S\,cm^{-1}$)	Stability	Refs.
NASICON-type $Li_{1.5}Al_{0.5}Ge_{1.5}(PO_4)_3$	10^{-6}–10^{-4}	10^{-9}	Sensitive to Li metal	[26–29,48,49]
NASICON-type $Li_{1.4}Al_{0.4}Ge_{0.2}Ti_{1.4}(PO_4)_3$	10^{-4}–10^{-3}	10^{-7}	Sensitive to Li metal	[30–32,48]
Garnet-type $Li_7La_3Zr_2O_{12}$:Al(0.9%)	10^{-4}	10^{-8}	Sensitive to H_2O and CO_2	[18–21,50–52]
Perovskite-type $Li_{3x}La_{2/3-x}TiO_3$ ($0.04 < x < 0.16$)	10^{-5}–10^{-3}	10^{-11}–10^{-9}	Sensitive to Li metal	[17,22,24,25,53]
Li_2S-P_2S_5 Li_3PS_4	10^{-4}–10^{-3}	10^{-9}–10^{-8}	Sensitive to H_2O	[34–36,52]
Li_2S-GeS_2-P_2S_5 $Li_{10}GeP_2S_{12}$	10^{-3}–10^{-2}	10^{-9}	Sensitive to H_2O and Li metal	[37–39,54]
Zeolite-based LiX zeolite membrane	10^{-4}	10^{-10}	Stable to H_2O, CO_2, and Li metal	[47]

perovskite and NASICON [48,53]; Ge-containing NASICON; lithium superionic conductor; and sulfide SEs [49,54,60], can be reduced when directly in contact with Li metal anodes. Meanwhile, the intermediate and terminal discharge products generated on the cathodes of metal-air or metal-sulfur batteries may also give rise to the decomposition of conventional SEs [61,62]. Thus, intensive studies focus on the construction of a stable interlayer between SEs and electrodes for protection [17,63,64]. Unfortunately, it may bring new problems, such as impeded interfacial ionic transport and a cumbersome preparation process. It is found that zeolites also exhibit high chemical and electrochemical stability to resist oxidation and reduction, which is beneficial for the stable operation of batteries [44,47,65].

B. Ion transport

Ionic transport in SEs is universally slower compared to liquid electrolytes, although inorganic SEs based on ion hopping may possess a competitive ionic conductivity (up to 1.2×10^{-2} $S\,cm^{-1}$) [37,61]. Therefore, steps to further improve the ionic conductivity of SEs have never slowed down. The doping strategy is regarded as a widely accepted approach to effectively improve the intrinsic ionic conductivity of SEs [66–68]. It is worth noting that element doping should be carefully conducted, because it may simultaneously increase the electronic conductivity of SEs, causing the formation of interior dendrites, the mechanism of which is elaborated in Sec. II C. Zeolites deliver a high intrinsic ionic conductivity of 2.4×10^{-2} $S\,cm^{-1}$ for a single crystal [47], showing a bright future as a new type of SEs.

Additionally, since conventional inorganic SEs are mostly prepared via pressing a powder into a pellet, inevitable grain boundaries and voids also increase the resistance for ion migration [69,70]. Sintering the SE pellets at high temperature with the assistance of sintering aids or filling the voids using fillers with high ionic conductivity (e.g., lithium nitride) can improved the ionic conductivity of SE pellets [71,72], while the hardly eliminated voids and instable fillers would be responsible for the limited effect. In comparison, compact zeolite membranes with thicknesses of only several micrometers can be prepared via a seed-assisted method [73,74], ensuring continuous ionic transport pathways, to achieve high conductivity.

C. Electron conduction

In a solid-state battery, SEs should also act as an electronically insulating separator to separate the cathode and the anode, avoiding the short circuiting of batteries. However, the relatively high electronic conductivity ($10^{-9} \sim 10^{-7}$ $S\,cm^{-1}$) of SEs would cause the formation of interior dendrites [52], and thus, increase the risk of the battery short circuiting, in spite of the high mechanical strength of these SEs to suppress dendrite growth on the surface of metal anodes. Specifically, lithium ions tend to be reduced by electrons and deposit inside the SEs with relatively facile electron mobility. Such a phenomenon is observed in solid-state batteries with LLZO [75], sulfide [76,77], and hydride SEs [78]. Furthermore, the nucleation of lithium inside SEs can be even worse because the electronic conductivity of SEs may ultimately increase during Li plating [79,80]. Introducing interstitial fillers or additives with low electronic conductivity is shown to be an effective countermeasure [72,81], while a short slab is also obvious as the compatibility of fillers or additives remains questionable. The low electronic conductivity (1.5×10^{-10} $S\,cm^{-1}$) of zeolite membranes with a tightly packed structure [47] fundamentally guarantees the safe operation of the battery by eliminating dendrite formation.

Overall, zeolites with superior chemical and electrochemical stability, high intrinsic and practical ionic conductivity, as well as low electronic conductivity can be considered as a promising choice for solid-state batteries. In addition, the excellent adaptability in various battery systems, enormous potential for large-scale production, as well as the low cost of raw materials and processing can further increase the competitiveness of zeolites in the future solid-state battery market.

III. EVOLUTION OF THE ROLE OF ZEOLITES IN SECONDARY BATTERIES

To gain a profound understanding of the advantages of zeolites in terms of stability, ionic transport, and side reaction suppression when applied in secondary batteries, we introduce the application of zeolites as functional layers, additives of composite SEs, and eventually inorganic SEs in this section.

A. Applications in constructing functional separators and layers

As common separators for lithium-ion batteries based on liquid electrolytes, polyethylene (PE) and polypropylene (PP) membranes unfortunately suffer from poor thermal stability, mechanical strength, and wettability, which affect the safety and performance of batteries. Inorganic materials, such as SiO_2 [82,83], Al_2O_3 [84–86], TiO_2 [87,88], etc. [89], are commonly employed for the optimization of separators. In comparison, zeolites, with a unique porous structure and tunable surface properties, are more favorable for improving the wettability of separators, in addition to having thermal and mechanical stability [90]. As a result, a zeolite-modified separator with superior wettability can achieve a high uptake of liquid electrolytes, which plays a key role in facile ionic transport [65]. It is worth mentioning that the wettability of zeolite-modified separators is closely related to the Si : Al ratio of the zeolites [91] and their surface roughness [65]. Meanwhile, the strong affinity toward polar solvent molecules, the trapping effect towards large-sized anions, and the unique pathways for lithium-ion transport also endow zeolite-modified separators with high ionic conductivity and lithium-ion transference number [92,93], which follows an analogous mechanism to that of the composite SEs and is discussed in Sec. III B. Owing to the high effective lithium-ion transport, batteries with zeolite-modified separators present an improved rate performance [Figs. 2(a) and 2(b)]. For comparison, the properties of separators modified by different inorganic materials and the corresponding performance of batteries are summarized in Table II.

Furthermore, the interfacial compatibility between separators and electrodes can be improved due to the superior adsorption and capture capability of zeolites towards impurities and byproducts dissolved in the electrolyte through intermolecular forces. Specifically, the zeolite can act as

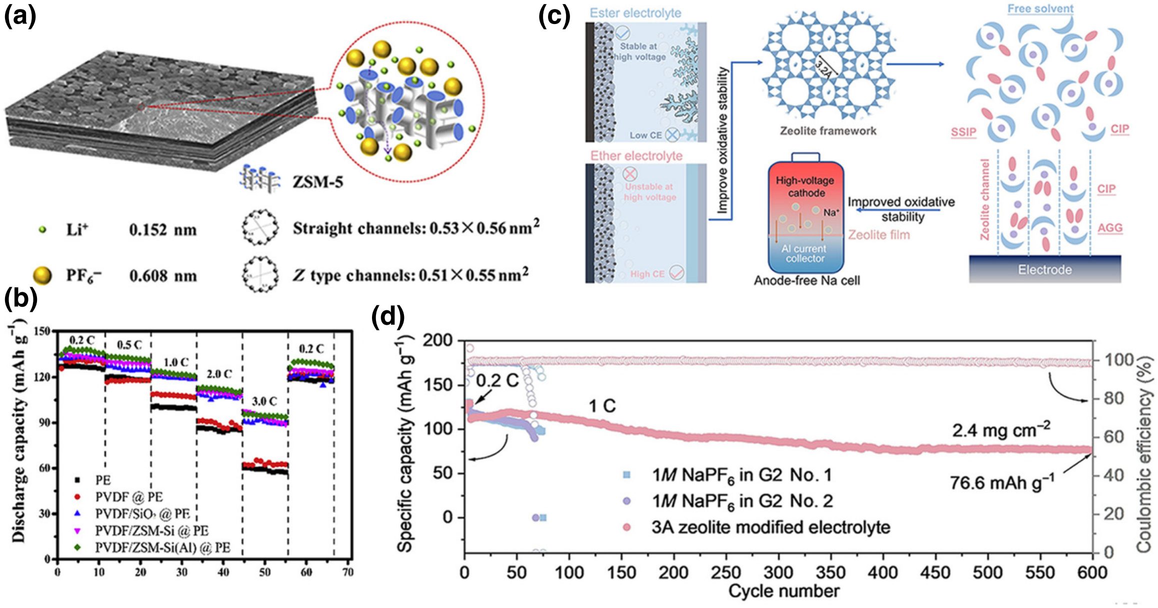

FIG. 2. Zeolite-based functional separators or layers. (a) Schematic illustration of the PE separator modified by ZSM-5, in which the proper pore size and unique channel structure of ZSM-5 contribute to facile lithium-ion conduction. (b) Rate capability of batteries with different separators. Specifically, the separator modified by Al-doped ZSM-5 with a Si : Al ratio of 40 exhibits the best rate performance. [93] Copyright 2017, Elsevier. (c) Construction path of Na batteries with a 3A zeolite molecular sieve film, in which the solvation structure of electrolytes can be regulated to avoid free solvent decomposition. (d) Cyclic stability of Na batteries using $NaPF_6$-diglyme (G2) with and without 3A zeolite film. Battery with 3A zeolite film shows a prolong lifespan of 600 cycles. [94] Copyright 2022, Wiley-VCH.

TABLE II. Properties of separators modified by different inorganic materials and the corresponding battery performance.

Substrate[a]	Additive	Thermal shrinkage	Electrolyte[b]	Electrolyte uptake (%)	Ionic conductivity ($\mathrm{S\,cm^{-1}}$)	Cathode (anode)	Capacity retention[c]	Rate capability	Refs.
P(VDF–TrFE)	Na*Y*		1 M $\mathrm{LiClO_4}$ in $\mathrm{3H_2O}$-PC	160–230	2.87×10^{-6}–3.54×10^{-7}				[90]
PET	NaA	<2% (170 °C,1.0 h)	1 M $\mathrm{LiPF_6}$ in EC/DEC = 1/1 (v/v)	194	2.1×10^{-3}	$\mathrm{LiFePO_4}$(Li)	98% (200 cycles)	0.26 mAh at 6C	[92]
PP	ZSM-5		1 M $\mathrm{LiPF_6}$ in EC/DEC/DMC = 1/1/1 ($v/v/v$)	168	5.2×10^{-4}	$\mathrm{Li_4Ti_5O_{12}}$(Li)		110 $\mathrm{mAh\,g^{-1}}$ at 1C	[91]
PE	ZSM-5	~0 (130 °C, 0.5 h)	1 M $\mathrm{LiPF_6}$ in EC/EMC/DEC = 1/1/1 ($w/w/w$)	430.9	5.4×10^{-4}	$\mathrm{LiCoO_2}$(Li)	94.2% (100 cycles at 0.2C)	100 $\mathrm{mAh\,g^{-1}}$ at 3C	[93]
PP	4A zeolite	14.4% (160 °C, 0.5 h)	1 M $\mathrm{LiPF_6}$ in EC/DEC/DMC = 1/1/1 ($v/v/v$)	270	2.25×10^{-3}	$\mathrm{LiFePO_4}$(Li)	96.2% (100 cycles)	~130 $\mathrm{mAh\,g^{-1}}$ at 2C	[65]
PI	ZSM-5	~0 (180 °C, 0.5 h)	1 M $\mathrm{LiPF_6}$ in EC/DMC =1/1 (v/v)	260	1.04×10^{-3}	$\mathrm{LiFePO_4}$(Li)	97.6% (50 cycles at 0.5C)	133 $\mathrm{mAh\,g^{-1}}$ at 2C	[44]
PET	$\mathrm{SiO_2}$	~0 (150 °C, 0.5 h)	1 M $\mathrm{LiPF_6}$ in EC/DEC = 1/1 (v/v)		9.1×10^{-4}	$\mathrm{LiCoO_2}$ (graphite)	~95% (100 cycles at 0.5C)	65 $\mathrm{mAh\,g^{-1}}$ at 2C	[82]
PE	$\mathrm{SiO_2}$	4.2% (120 °C, 0.5 h)	1 M $\mathrm{LiPF_6}$ in EC/DEC = 1/1 (v/v)		8.4×10^{-4}	$\mathrm{LiFePO_4}$(Li)	~100% (200 cycles at 0.2C)	65 $\mathrm{mAh\,g^{-1}}$ at 5C	[83]
PE	$\mathrm{Al_2O_3}$	7.6% (105 °C, 1.0 h)	1 M $\mathrm{LiPF_6}$ in EC/DEC = 1/1 (v/v)	237.8	8.1×10^{-4}	$\mathrm{LiCoO_2}$ (mesocarbon microbeads)	~86% (200 cycles at 0.5C)	~120 $\mathrm{mAh\,g^{-1}}$ at 2C	[84]
PP	$\mathrm{Al_2O_3}$	10% (150 °C, 0.5 h)	1 M $\mathrm{LiPF_6}$ in EC/DEC = 1/1 (v/v)		9.5×10^{-4}	$\mathrm{LiMn_2O_4}$ (graphite)	~97% (350 cycles at 0.5C)		[85]
PE	$\mathrm{Al_2O_3}$	~0 (150 °C, 0.5 h)	1 M $\mathrm{LiPF_6}$ in EC/DEC/DMC = 1/1/1 ($v/v/v$)		5.3×10^{-4}	$\mathrm{LiFePO_4}$ (graphite)	85.6% (100 cycles at 1C)	~80 $\mathrm{mAh\,g^{-1}}$ at 5C	[86]
PP	$\mathrm{TiO_2}$	20% (160 °C, 0.5 h)	1 M $\mathrm{LiPF_6}$ in EC/DEC = 1/1 (v/v)	144.3	4.8×10^{-4}	$\mathrm{LiCoO_2}$(Li)	84% (100 cycles at 0.5C)	~72 $\mathrm{mAh\,g^{-1}}$ at 8C	[87]
PE	$\mathrm{TiO_2}$	36% (150 °C, 0.5 h)	1 M $\mathrm{LiPF_6}$ in EC/DEC/DMC = 1/1/1 ($v/v/v$)		5.0×10^{-4}	$\mathrm{LiFePO_4}$(Li)	~100% (100 cycles at 0.3C)	~67 $\mathrm{mAh\,g^{-1}}$ at 5C	[88]
PE	$\mathrm{ZrO_2}$	~60% (150 °C, 1.0 h)	1 M $\mathrm{LiPF_6}$ in EC/EMC = 3/7 (v/v)	~130	6.1×10^{-4}	$\mathrm{LiCoO_2}$(Li)	95% (50 cycles at 0.5C)		[89]

[a] P(VDF-TrFE) is the abbreviation for poly(vinylidene fluoride-trifluoroethylene); PET is the abbreviation for polyethylene terephthalate; and PI is the abbreviation for polyimide.

[b] PC is the abbreviation for propylene carbonate; EC is the abbreviation for ethylene carbonate; DEC is the abbreviation for diethyl carbonate; DMC is the abbreviation for dimethyl carbonate; and EMC is the abbreviation for ethyl methyl carbonate.

[c] 1C rate means that it takes 1 h for the cell to drain in a predefined voltage window.

a trace water adsorbent and hydrofluoric acid (byproducts from the side reaction between $LiPF_6$-based electrolyte and trace water) scavenger to suppress the dissolution of transition metal ions in cathode materials, resulting in an enhanced Coulombic efficiency (CE) of the full cell [95]. The electrochemical stability of batteries can be further improved due to the construction of functional zeolite layers on electrodes. Recently, Zhou's group proposed a novel electrolyte sieving strategy to suppress the decomposition of liquid electrolyte [94,96,97]. The solvation structure of the electrolyte can be effectively regulated owing to the pore structure of the zeolite, resulting in a prolonged cycle life of batteries with a high CE [Figs. 2(c) and 2(d)].

B. Application as the additives of composite SEs

As mentioned above, polymer SEs are easily penetrated by the dendrite due to their intrinsic softness and usually deliver a lower ionic conductivity in comparison with inorganic SEs [61]. To solve these problems, inorganic additives, including inert fillers (SiO_2, Al_2O_3, TiO_2, etc.) [98–100] and active fillers with ionic conductive capability (perovskite-, NASICON-, and garnet-type ceramics) [101–104], are introduced to prepare composite SEs. In general, the introduction of inorganic fillers inhibits the crystallization of polymer chains, which unlocks their segmental motion to facilitate ion transport [104]. Additionally, the Lewis acid-base interaction between inert fillers and ions of salts is beneficial for the dissociation of the salt, leading to the improved ionic conductivity [105].

According to the above mechanism for improving the ionic conductivity of polymer SEs, zeolites emerge as a more promising candidate owing to their tunable porous structure and abundant Lewis acid sites. Xi *et al.* investigated the role of zeolites in a composite SE composed of PEO as the polymer matrix, $LiClO_4$ as the Li salt, and ZSM-5 as the filler for the first time [106]. The addition of zeolites increases the ratio of amorphous PEO that is favorable for facile Li^+ transport. Meanwhile, the stronger Lewis acid sites, compared with SiO_2 and Al_2O_3, on the surface and inside the channels of ZSM-5 lead to a higher

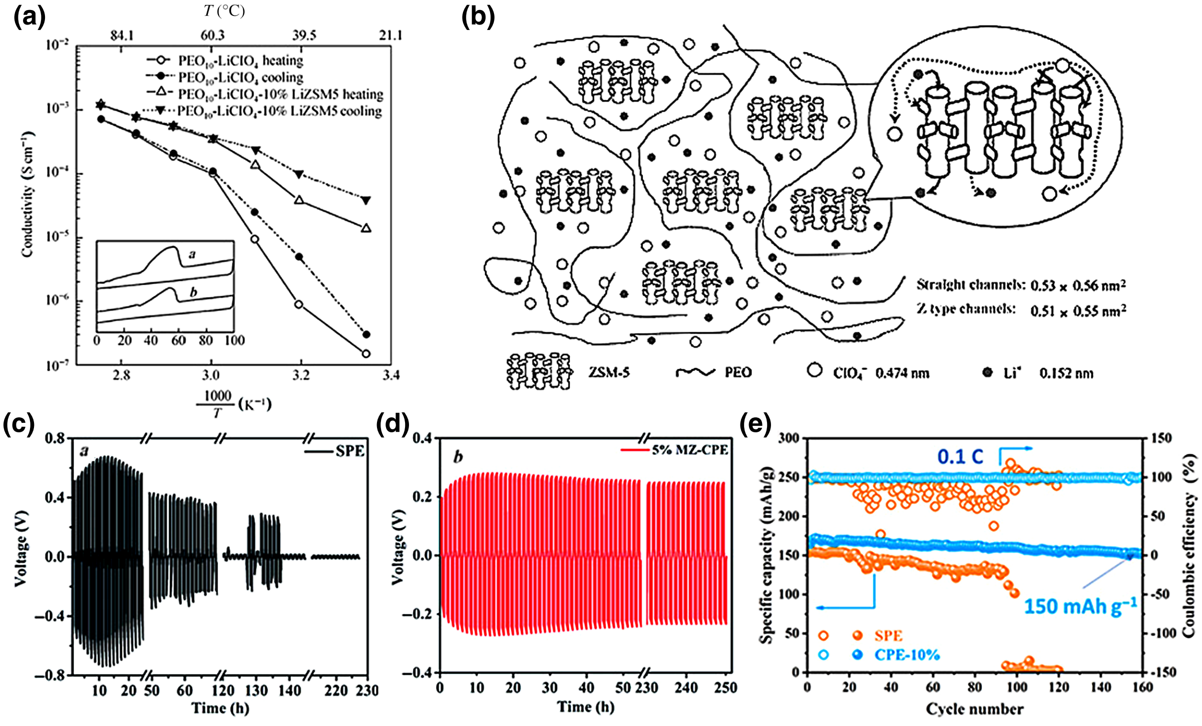

FIG. 3. Zeolite-based additives in composite SEs. (a) Ionic conductivities of polymer SEs and composite SEs with 10% LiZSM-5; inset shows the corresponding differential scanning calorimetry curves. Ionic conductivities of composite SEs with 10% LiZSM-5 are much higher than those of polymer SE. [106] Copyright 2004, Springer Nature. (b) Schematic representation of selective passage of Li^+ by ZSM-5 in composite SEs. Pore sizes of ZSM-5 prefer the direct passage of relatively small Li^+ rather than ClO_4^- due to the size effect and electrostatic interactions. [107] Copyright 2004, American Chemical Society. Cycling performance of lithium symmetric cell with polymer SEs (c) and zeolite-modified SEs (d). Battery with zeolite-modified SEs exhibits superior cycling stability due to the stability and compatibility of composite SEs against Li metal anodes. [108] Copyright 2021, Royal Society of Chemistry. (e) Cycling performance of $LiFePO_4$/Li batteries using polymer SEs and zeolite-modified composite SEs. Battery with zeolite-modified SEs presents a superior cycling performance due to fast ionic transport and excellent interfacial compatibility of zeolite-modified SEs. [109] Copyright 2018, American Chemical Society.

TABLE III. Properties of composite SEs with various additives, including zeolites.

Fillers	Polymer[a]	Salt[b]	Ionic conductivity ($S\,cm^{-1}$)	t_{Li^+}	Refs.
	PEO	$LiClO_4$	1.5×10^{-7} at 25 °C	0.196 at 40 °C	[106]
ZSM-5 (MFI)	PEO	$LiClO_4$	1.4×10^{-5} at 25 °C	0.36 at 40 °C	[106,107,110,111]
Na*Y* (FAU)	PEO	$LiClO_4$	10^{-4} at 60 °C 10^{-5} at 25 °C	0.27	[110]
Beta (BEA)	PEO	$LiClO_4$	10^{-4} at 60 °C 10^{-5} at 25 °C	0.28	[110]
SSZ-13 (CHA)	PEO	LiTFSI	1.91×10^{-3} at 60 °C; 4.43×10^{-5} at 20 °C	0.5 at 60 °C	[109]
Na*Y* (FAU)	PEO	LiTFSI	1.66×10^{-2} at 60 °C		[112]
SSZ-13 (CHA)	PEO	LiTFSI	5.34×10^{-2} at 70 °C	0.85 at 60 °C	[108]
SiO_2	PEO	$LiClO_4$	7.2×10^{-6} at 25 °C	0.24 at 40 °C	[106]
SiO_2	PEO	$LiClO_4$	1.5×10^{-4} at 25 °C	0.54 at 25 °C	[98]
Al_2O_3	PEO	$LiClO_4$	9.7×10^{-6} at 25 °C	0.251 at 40 °C	[106]
TiO_2	PEO	$LiClO_4$	10^{-4} at 60 °C 10^{-6} at 25 °C	0.47 at 80 °C	[99]
TiO_2	PEGMEM-SMA	LiTFSI	1.1×10^{-4} at 30 °C	0.37 at room temperature	[100]
SO_4^{2-}-ZrO_2	PEO	$LiClO_4$		0.29 at 70 °C	[107]
$Li_{1.5}Al_{0.5}Ge_{1.5}(PO_4)_3$	PEO	LiTFSI	6.76×10^{-4} at 60 °C	0.378 at 60 °C	[101]
$Li_{1.5}Al_{0.5}Ti_{1.5}(PO_4)_3$	PEO	LiTFSI	1×10^{-4} at 30 °C	0.37 at 60 °C	[102]
$Li_7La_3Zr_2O_{12}$	PVDF	$LiClO_4$	2.6×10^{-4} at 25 °C	0.682	[103]

[a] PEGMEM is the abbreviation for poly(ethylene glycol) methyl ether methacrylate and SMA is the abbreviation for stearyl methacrylate.

[b] LiTFSI is the abbreviation for lithium bis(trifluoromethane)sulfonimide.

improvement of ionic conductivity [Fig. 3(a)]. Notably, an excess amount of zeolites can conversely reduce the ionic conductivity of composite SEs due to the blocking effect [110]. In addition to the ionic conductivity, the lithium-ion transference number (t_{Li^+}) of composite SEs increases simultaneously for multiple reasons [107]. (1) The Lewis acid-base interactions between ZSM-5 and the oxygen of PEO and/or ClO_4^- give rise to the release of more mobile Li^+. (2) The specific pore size of ZSM-5 and the electrostatic force lead to the facile passage of Li^+ rather than ClO_4^-, as shown in Fig. 3(b). (3) The ion-exchange capability of ZSM-5 provides an extra possibility for Li^+ conduction. The validity of the strategy that introduces zeolites as the filler of composite SEs is demonstrated by using zeolites with different topological structures, such as MFI, FAU, BEA, and CHA [109,110], and a detailed comparison is summarized in Table III. It seems that SSZ-13 (CHA) presents the best capability to enhance the ionic conductivity and t_{Li^+} of composite SEs owing to an adsorption effect towards Li^+. However, the morphology, dispersity, channel structure, pore size, and Si : Al ratio of zeolite fillers, which essentially impact on ionic transport in composite SEs, were not precisely controlled in previous works. Thus, a judgment cannot be made arbitrarily, and further discussion is provided in the next section.

In addition to ionic conductivity and t_{Li^+}, thermal stability and the mechanical strength of polymer SEs can be further improved by the addition of zeolites [109,111,112]. The robust cross-link interaction between zeolites and polymers will broaden the voltage window of SEs [109]. Moreover, the stability and compatibility of SEs against Li metal anodes can be enhanced [Figs. 3(c) and 3(d)]; this is attributed to the adsorption of residual solvents or trace water in a polymer matrix [108] and the regulation of lithium deposition behavior [112] by zeolites. Benefiting from the comprehensive properties of zeolites, batteries with zeolite-modified composite SEs display superior cycling performance [Fig. 3(e)].

C. Application as inorganic SEs

Actually, research on the ionic conduction of zeolites began in the last century [113–115], despite the lack of studies focusing on zeolites as inorganic SEs. In general, framework-associated cations (e.g., alkali ions) for charge balancing are perceived as the mobile charge carriers in aluminosilicate zeolites, and their content depends on the content of Al atoms in zeolite frameworks [116]. Therefore, zeolites with a lower Si : Al ratio will serve as good ionic conductors in light of the high content of framework-associated cations. However, the ionic conductivity of

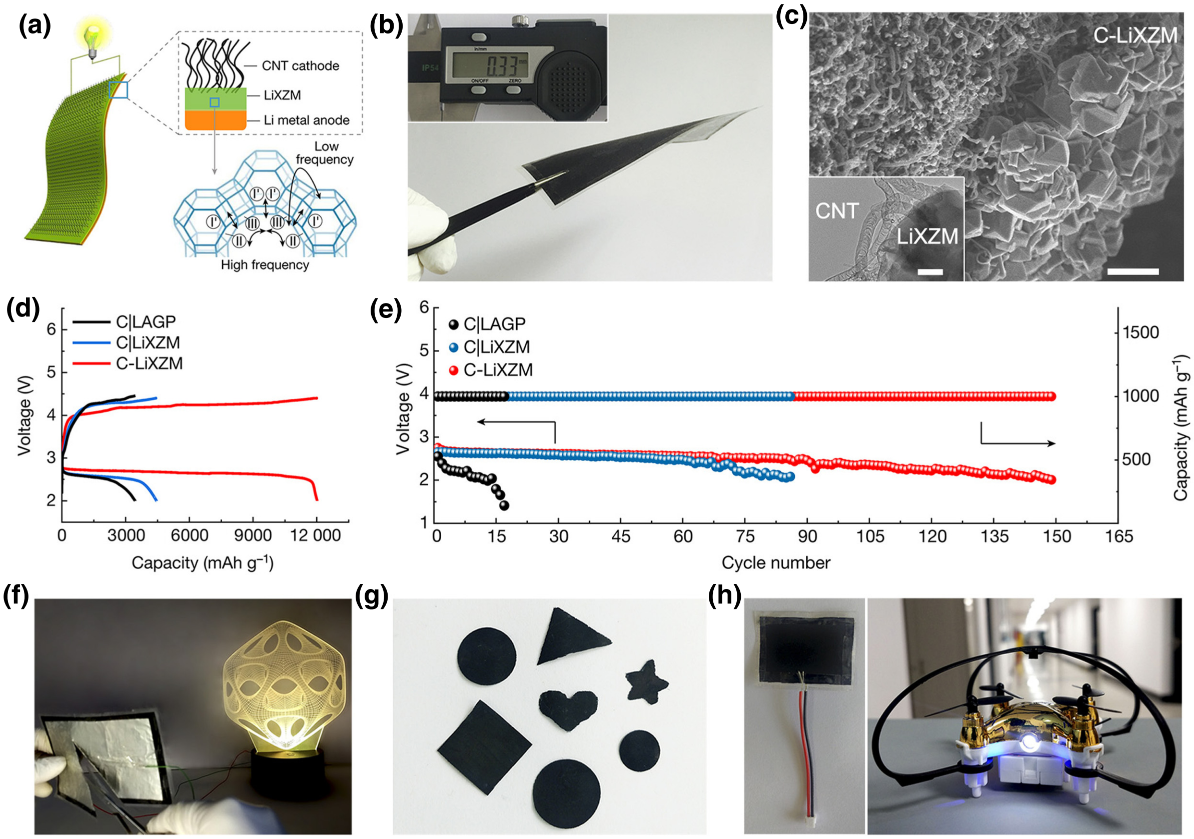

FIG. 4. Zeolite-based inorganic SE. (a) Schematic of the solid-state Li-air battery (SSLAB) with a cathode-integrated LiXZM, and the conduction mechanism of Li ions in Li*X* zeolite. (b) Photograph of a SSLAB with a cathode-integrated LiXZM. (c) Scanning electron microscopy and transmission electron microscopy images of the cathode-integrated LiXZM. (d) Specific capacities of SSLABs with a cathode-integrated LiXZM (C-LiXZM), a nonintegrated LiXZM (C|LiXZM), and LAGP (C|LAGP). (e) Corresponding cycling performance of solid-state Li-air batteries upon cycling. (f) Safety property of SSLAB with a cathode-integrated LiXZM. (g) Flexible shape tailoring of the SSLAB with a cathode-integrated LiXZM. (h) Unmanned aerial vehicle powered by a SSLAB with a cathode-integrated LiXZM. [47] Copyright 2021, Springer Nature.

zeolite pellets, which are prepared by a common pressing method for the preparation of SEs [69], is too low, even at a high temperature [113,114]. This is possibly related to insufficient physical contact between zeolite particles in ceramic pellets, and thus, the zeolite pellets reported in previous studies are unsatisfactory for application as SEs.

As a breakthrough, our group developed a Li*X* zeolite membrane (LiXZM) as a solid electrolyte for Li-air batteries [Fig. 4(a)] [47]. Taking advantage of the continuous pathways for lithium-ion migration, a homogeneous ultrathin LiXZM shows a sufficiently high ionic conductivity of 2.7×10^{-4} S cm^{-1}, which is far beyond that of the Li*X* zeolite pellet (3.3×10^{-9} S cm^{-1}). Furthermore, the low electronic conductivity of LiXZM (1.5×10^{-10} S cm^{-1}) fundamentally inhibits the nucleation of lithium inside the LiXZM, preventing the formation of interior lithium dendrites based on the mechanism mentioned in the previous section. Furthermore, the intrinsic high chemical and electrochemical stability of LiXZM effectively prevents electrolyte degeneration under the attack of air, reactive oxygen species, and hyperactive Li anode, which consequently eliminates the negative effect derived from byproducts and achieves a broad voltage window of 0–7 V. Combined with the desirable design of an integrated battery structure [Figs. 4(b) and 4(c)], the Li-air battery with the LiXZM delivers a high discharge specific capacity [12 020 mAh g^{-1}, Fig. 4(d)] and a prolonged cycling life [149 cycles, Fig. 4(e)] in ambient air. This cycling life is much higher than those of commercial lithium aluminum germanium phosphate (LAGP) based batteries (max. 27 cycles) and even superior to those of batteries containing organic liquid electrolytes (max. 102 cycles) under the same conditions. In addition, superior flexibility, shape-tailoring capability, and environmentally friendly production also endow the zeolite-based solid-state Li-air batteries with practical applicability [Figs. 4(f)–4(h)].

Inspired by the confinement effect of zeolites towards guest species [40], our group further introduces ionic species into the channel of zeolites to regulate the ionic transport behavior via the interaction between guest ionic species and the zeolite host. This host-guest assembly strategy provides a new insight into the development of SEs with fast ionic conduction and will be detailed in our future work.

IV. FUTURE PERSPECTIVE OF ZEOLITE-BASED SES

Although zeolites display great potential, research on zeolite-based SEs is still in its infancy, and comprehensive investigations should be carried out from multiple perspectives (Fig. 5).

A. Design and regulation of materials

The topological structure, chemical composition, and host-guest interaction should be carefully considered for the development of zeolite-based SEs. First of all, the channel structure and pore size of zeolites, which vary with topological structures, might significantly impact on ion transport in zeolite frameworks. According to

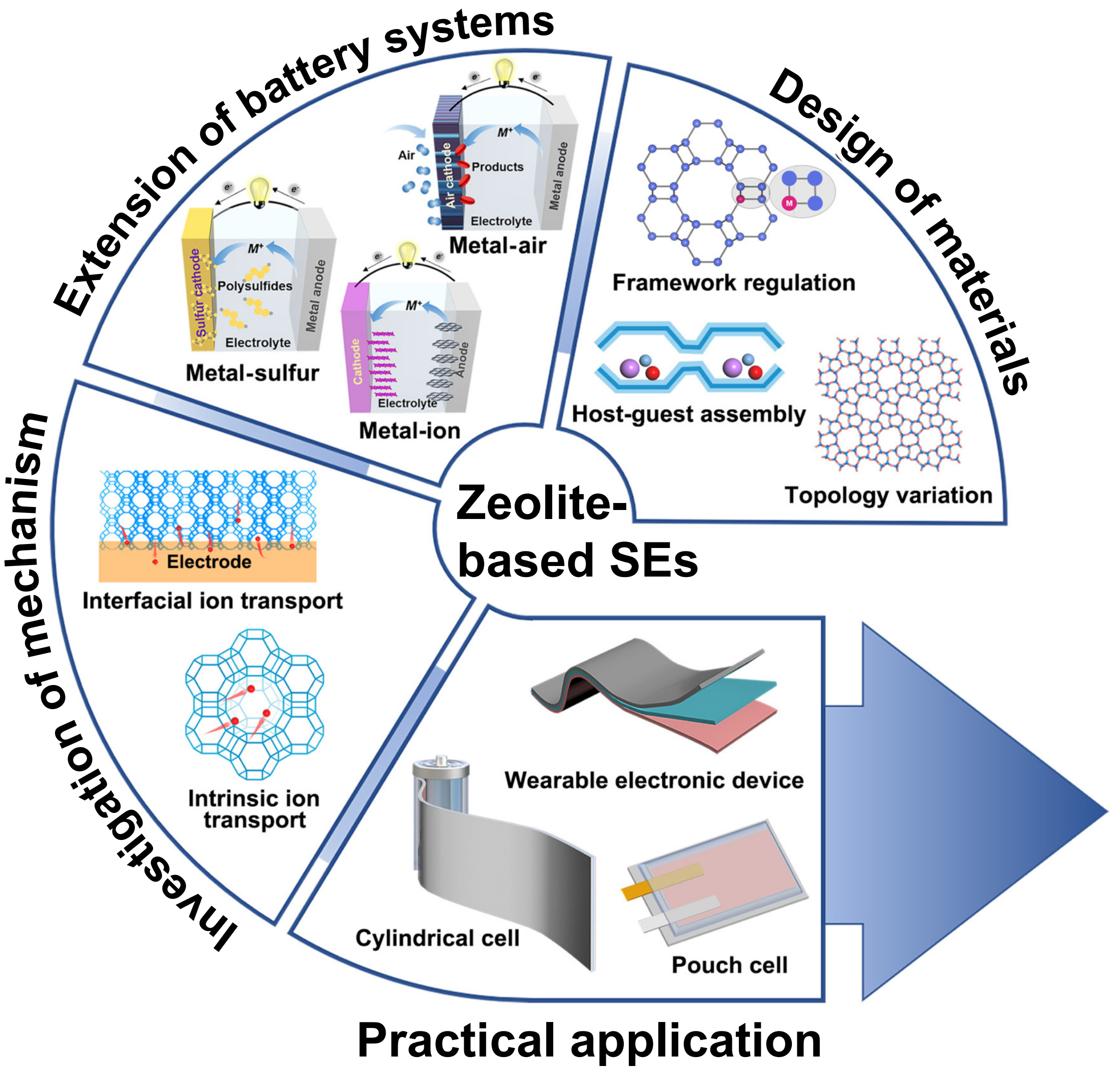

FIG. 5. Future perspective of zeolite-based SEs. Schematic illustration of the development directions for zeolite-based electrolytes. First, the design of zeolite-based SEs can be carried out through the selection of different topological structures, regulation of frameworks, and the introduction of functional guest species in pores. Second, zeolite-based SEs present a promising application in various battery systems because of their capabilities in ion exchange, adsorption, and separation. Third, the investigation of both intrinsic and interfacial ion transport mechanisms is essential for the development of zeolite-based SEs and the fabrication of high-efficiency solid-state batteries. Finally, the adaptability of zeolite-based SEs for various practical applications should be improved via technology optimization.

previous reports, analcime (ANA), which possesses a uniform one-dimensional channel structure without pronounced potential wells, provides a more facile migration pathway for Li^+ and Na^+ than sodalite (SOD), with three-dimensional channels. However, NaA zeolite (LTA) with a three-dimensional channel structure delivers a higher ionic conductivity than that of analcime, indicating that there are other factors affecting the ionic conduction of zeolites than the channel structure. The pore size of the zeolite is another key factor for ionic conduction, as the size of cages and corresponding windows should be large enough to allow the facile migration of mobile cations. Specifically, open frameworks with larger cages (e.g., Y zeolite with FAU structure) provide a facile pathway for cation migration, while ion migration in zeolites like ZSM-5 (MFI) may be hindered due to the repulsion effect between cations [115]. On the other hand, the overlarge pore size of zeolites compared to mobile cations will lead to a higher electrostatic interaction between mobile cations and the framework, resulting in the immobilization of framework-associated cations [113,117]. Therefore, appropriate channels and pore sizes for ion migration are the prerequisites for high-performance zeolite-based SEs.

In addition, the chemical composition of zeolites is another important factor for the design of zeolite-based SEs. As mentioned above, the content of mobile cations is highly related to the Si : Al ratio of zeolites. Reducing the Si : Al ratio is an effective approach to increase the density of mobile cations in zeolites, which is favorable for improving the ionic conductivity, according to the Arrhenius relationship:

$$\sigma = qnu,$$

where σ is the ionic conductivity of materials, and q, n, and u represent the charge, concentration, and mobility of charge carriers, respectively [69]. Meanwhile, the sites with low activation energy are more likely to be occupied in zeolites with a lower Si : Al ratio [118], and the mobility of mobile cations is consequently increased. A typical case is the LiX zeolite with the lowest Si : Al ratio of 1.0 [119], which also possesses an open framework with appropriate channels for ion conduction. It is worth mentioning that superior ionic conductivity is not always achieved in the zeolite with a lower Si : Al ratio due to steric effects and electrostatic repulsion originating from mobile cations with a large ionic radius. For instance, the best ionic conductivity of offretite (OFF) is obtained from the sample with a Si : A1 ratio of 3.0 when the charge carriers are K^+ or Rb^+. Also, the cation-cation interaction should be considered to reduce the repulsive force towards mobile cations when regulating the framework composition [118,120].

Furthermore, introducing guest species into zeolite hosts may also be an effective approach to fabricate multifunctional SEs for solid-state batteries. Our recent work demonstrates that ionic species confined in the zeolite channels will interact with the framework-associated cations, and thus, boost the effective ionic conduction of electrolytes.

B. Extension of solid-state battery systems

Alkali metal ions, and even other multivalent ions, can occupy the mobile framework-associated sites of zeolites via ion exchange [114,121–123]. Thus, the application of zeolite-based SEs is highly anticipated in various energy storage devices, especially post-lithium-ion batteries, such as sodium-ion batteries and potassium-ion batteries. Our group preliminarily demonstrated the validity of zeolite-based SEs for sodium-ion batteries in follow-up work, and further efforts should be devoted to other battery systems. It is worth noting that the type of mobile cations also affects the ionic conductivity of zeolites with the same topological structure, which is acceptable due to the different ionic radii of charge carriers and different electrostatic interactions. For example, Li cancrinite, Na cancrinite, and K cancrinite show distinct ionic conductivities of 3.9×10^{-5}, 1.5×10^{-3}, and 1.0×10^{-4} $\mathrm{S\,cm^{-1}}$ at 400 °C, respectively [114].

In addition to metal-ion batteries, zeolite-based SEs are also compatible with batteries using metal anodes, such as metal-sulfur batteries and metal-air batteries. The adsorption and separation capabilities of zeolites provide unique superiority to scavenge trace water, as mentioned in Sec. III [108,109], preventing the metal anode from corroding. Also, the porous structure of zeolites is favorable for homogenizing lithium-ion flux by lowering the interfacial ionic transport resistance and slowing down the consumption of lithium ions [124], and thus, regulating the metal deposition behavior to suppress dendrite formation. In particular, the stability of zeolites against air, lithium metal, and intermediate and terminal discharge products (detailed in Sec. II) provides great advantages for the stable operation of lithium metal batteries with high energy density compared with conventional SEs.

C. Comprehensive investigation of ion transport mechanism

Ionic conduction in zeolites is achieved via a hopping process, which is similar to other inorganic crystalline materials. Taking NaA zeolite (LTA) as an example, the framework-associated cations at site II (near the eight-ring windows) and site III (near the four-ring windows) are the predominant contributors to ionic diffusion via a concerted transposition process between site II and site III [125]. As for the zeolites with FAU structure (e.g., X and Y zeolite), local charge transport and long-range order ionic diffusion occur simultaneously; these originate from the migration of framework-associated cations at site II (near the six-ring windows inside supercages) and site III (near the four-ring windows inside supercages) [118]. Although the ion transport behavior in the specific type of zeolites is preliminarily studied, it is essential to provide an in-depth illustration of the ionic pathways in zeolites to optimize the properties of zeolite-based SEs, and thus, improve the performance of batteries. Similar studies are achieved for the design of conventional SEs. Wang *et al.* [126] investigated the impact of anion sublattices on the ionic conductivity of sulfide SEs, and thus, developed specific criteria to look for better conductors. Culver *et al.* [127] summarized the structural requirements for achieving high ionic conductivities and emphasized the importance of optimizing the electrode-SE interface. Additionally, the revelation of an interfacial ionic transport mechanism triggered intensive studies on interfacial modification to reduce interfacial impedance [51,128–134]. Thus, further clarification of ion transport behavior in zeolites at the atomic level is necessary to provide the basis for the selection and regulation of zeolite-based SEs, and the interfacial ion conduction mechanism is another key area of concern to achieve the practical operation of zeolite-based SEs at the device level.

To investigate the ion conduction mechanism of zeolites, advanced *in situ* and *ex situ* characterization techniques are highly necessary, accompanied by the employment of traditional characterization methods [69, 119,135–139], such as nuclear magnetic resonance, electrochemical impedance spectroscopy, and electron microscopy. In parallel, computer simulation is another powerful tool to depict the dynamic procedure for ion transport. The energy barriers and pathway for ion diffusion in SEs can be investigated via first-principles calculations based on quantum mechanics combined with the nudged elastic band method, while the initial and final states of mobile ions must be input [140,141]. In addition, molecular dynamics simulation is another computational method to study the ion diffusion behavior based on classical mechanics [142–144], which is used to reveal the ionic diffusion mechanism in zeolites. To access more complex systems, *ab initio* molecular dynamics simulation emerges to quantify detailed diffusion behavior [144–146] and shows great potential to aid in the design and optimization of zeolite-based SEs.

D. Optimization of processing technologies for practical application

Although the industrial production of zeolites is achieved, the large-scale production of zeolite-based SEs with low cost, high quality, and energy conservation remains a challenge. As mentioned in Sec. II, the inevitable voids between the rigid solid particles of inorganic SEs, which are commonly prepared via a pressing method, is one of the main culprits for impeding ion conduction and inducing interior dendrite formation. Beyond the unsatisfactory conventional preparation strategies, the fabrication of zeolite membranes with dense features via a seed-assisted method seems like a judicious choice. The preparation of zeolite membranes with different topological structures, including MFI, LTA, CHA, and FAU, is reported [147–152], laying the foundation for the development of zeolite-based SEs. However, the selection of substrates for zeolite membranes should be made cautiously to ensure the integrity of membranes, achieve the high energy density of batteries, and even adapt flexible solid-state devices. For example, polymer- or carbon-based substrates might be promising choices owing to their light weight and flexibility. Physical contact between SEs and electrodes should also be improved to achieve a high electrochemical performance. To this end, composite cathodes consisting of active materials and SE particles are generally prepared for conventional solid-state batteries [153–155], while the *in situ* fabrication strategy for the zeolite-based SE-electrode integrated structure provides the possibility to construct an interface with lower contact impedance. Furthermore, the compatibility of zeolite-based electrolytes with battery assembly strategies for traditional battery packs (such as cylinder cells and pouch cells), wearable devices, and microbatteries remains to be verified before commercialization.

In view of their impressive stability, ionic conductivity, and electronic insulation, zeolites are full of promise to take up the baton from traditional SEs in solid-state batteries and open up enormous possibilities in the fields of material design, battery system expansion, mechanism investigations, and industrialization for zeolite-based SEs.

ACKNOWLEDGMENT

We thank the National Natural Science Foundation of China (Grants No. 22288101, No. 21920102005, and No. 21835002) and the 111 Project (Grant No. B17020) for supporting this work.

[1] M. Armand and J. M. Tarascon, Building better batteries, Nature **451**, 652 (2008).

[2] B. Dunn, H. Kamath, and J. M. Tarascon, Electrical energy storage for the grid: A battery of choices, Science **334**, 928 (2011).

[3] M. S. Whittingham, History, evolution, and future status of energy storage, Proc. IEEE **100**, 1518 (2012).

[4] J. Xu, J. Ma, Q. Fan, S. Guo, and S. Dou, Recent progress in the design of advanced cathode materials and battery models for high-performance lithium-X ($X = O_2$, S, Se, Te, I_2, Br_2) batteries, Adv. Mater. **29**, 1606454 (2017).

[5] R. Chen, R. Luo, Y. Huang, F. Wu, and L. Li, Advanced high energy density secondary batteries with multi-electron reaction materials, Adv. Sci. **3**, 1600051 (2016).

[6] F. Cheng, J. Liang, Z. Tao, and J. Chen, Functional materials for rechargeable batteries, Adv. Mater. **23**, 1695 (2011).

[7] Y. Ding, Z. P. Cano, A. Yu, J. Lu, and Z. Chen, Automotive Li-ion batteries: Current status and future perspectives, Electrochem. Energy Rev. **2**, 1 (2019).

[8] C.-X. Zu and H. Li, Thermodynamic analysis on energy densities of batteries, Energy Environ. Sci. **4**, 2614 (2011).

[9] M. M. Thackeray, C. Wolverton, and E. D. Isaacs, Electrical energy storage for transportation—approaching the limits of, and going beyond, lithium-ion batteries, Energy Environ. Sci. **5**, 7854 (2012).

[10] J. Betz, G. Bieker, P. Meister, T. Placke, M. Winter, and R. Schmuch, Theoretical versus practical energy: A plea for more transparency in the energy calculation of different rechargeable battery systems, Adv. Energy Mater. **9**, 1803170 (2019).

[11] Y. Liu, P. He, and H. Zhou, Rechargeable solid-state Li–air and Li–S batteries: Materials, construction, and challenges, Adv. Energy Mater. **8**, 1701602 (2018).

[12] C. Yang, K. Fu, Y. Zhang, E. Hitz, and L. Hu, Protected lithium-metal anodes in batteries: From liquid to solid, Adv. Mater. **29**, 1701169 (2017).

[13] Y. An, X. Han, Y. Liu, A. Azhar, J. Na, A. K. Nanjundan, S. Wang, J. Yu, and Y. Yamauchi, Progress in solid polymer electrolytes for lithium-ion batteries and beyond, Small **18**, 2103617 (2022).

[14] J. Wan, J. Xie, X. Kong, Z. Liu, K. Liu, F. Shi, A. Pei, H. Chen, W. Chen, J. Chen, *et al.*, Ultrathin, flexible, solid polymer composite electrolyte enabled with aligned nanoporous host for lithium batteries, Nat. Nanotechnol. **14**, 705 (2019).

[15] Y. Cui, J. Wan, Y. Ye, K. Liu, L. Y. Chou, and Y. Cui, A fireproof, lightweight, polymer–polymer solid-state electrolyte for safe lithium batteries, Nano Lett. **20**, 1686 (2020).

[16] D. Cao, X. Sun, Q. Li, A. Natan, P. Xiang, and H. Zhu, Lithium dendrite in all-solid-state batteries: Growth mechanisms, suppression strategies, and characterizations, Matter **3**, 57 (2020).

[17] Z. Gao, H. Sun, L. Fu, F. Ye, Y. Zhang, W. Luo, and Y. Huang, Promises, challenges, and recent progress of inorganic solid-state electrolytes for all-solid-state lithium batteries, Adv. Mater. **30**, 1705702 (2018).

[18] R. Murugan, V. Thangadurai, and W. Weppner, Fast lithium ion conduction in garnet-type $Li_7La_3Zr_2O_{12}$, Angew. Chem. Int. Ed. **46**, 7778 (2007).

[19] E. Rangasamy, J. Wolfenstine, and J. Sakamoto, The role of Al and Li concentration on the formation of cubic garnet solid electrolyte of nominal composition $Li_7La_3Zr_2O_{12}$, Solid State Ionics **206**, 28 (2012).

[20] J. Wolfenstine, J. Ratchford, E. Rangasamy, J. Sakamoto, and J. L. Allen, Synthesis and high Li-ion conductivity of Ga-stabilized cubic $Li_7La_3Zr_2O_{12}$, Mater. Chem. Phys. **134**, 571 (2012).

[21] Y. Zhu, S. Wu, Y. Pan, X. Zhang, Z. Yan, and Y. Xiang, Reduced energy barrier for Li^+ transport across grain boundaries with amorphous domains in LLZO thin films, Nanoscale Res. Lett. **15**, 153 (2020).

[22] Y. Inaguma, L. Chen, M. Itoh, and T. Nakamura, High ionic conductivity in lithium lanthanum titanate, Solid State Commun. **86**, 689 (1993).

[23] Y. Inaguma, L. Chen, M. Itoh, and T. Nakamura, Candidate compounds with perovskite structure for high lithium ionic conductivity, Solid State Ionics **70–71**, 196 (1994).

[24] J. Z. Lee, Z. Wang, H. L. Xin, T. A. Wynn, and Y. S. Meng, Amorphous lithium lanthanum titanate for solid-state microbatteries, J. Electrochem. Soc. **164**, A6268 (2017).

[25] Y. Huang, L. He, and X. Zhu, Low temperature synthesis of $Li_{0.33}La_{0.55}TiO_3$ solid electrolyte with Al^{3+} doping by a modified Pechini method, Ionics **28**, 1739 (2022).

[26] J. K. Feng, L. Lu, and M. O. Lai, Lithium storage capability of lithium ion conductor $Li_{1.5}Al_{0.5}Ge_{1.5}(PO_4)_3$, J. Alloys Compd. **501**, 255 (2010).

[27] C. R. Mariappan, C. Yada, F. Rosciano, and B. Roling, Correlation between micro-structural properties and ionic conductivity of $Li_{1.5}Al_{0.5}Ge_{1.5}(PO_4)_3$ ceramics, J. Power Sources **196**, 6456 (2011).

[28] Z. Sun, L. Liu, Y. Lu, G. Shi, J. Li, L. Ma, J. Zhao, and H. An, Preparation and ionic conduction of $Li_{1.5}Al_{0.5}Ge_{1.5}(PO_4)_3$ solid electrolyte using inorganic germanium as precursor, J. Eur. Ceram. Soc. **39**, 402 (2019).

[29] S. V. Pershina, B. D. Antonov, A. S. Farlenkov, and E. G. Vovkotrub, Glass-ceramics in $Li_{1+x}Al_xGe_{2-x}(PO_4)_3$ system: The effect of Al_2O_3 addition on microstructure, structure and electrical properties, J. Alloys Compd. **835**, 155281 (2020).

[30] P. Zhang, H. Wang, Y.-G. Lee, M. Matsui, Y. Takeda, O. Yamamoto, and N. Imanishi, Tape-cast water-stable NASICON-type high lithium ion conducting solid electrolyte films for aqueous lithium-air batteries, J. Electrochem. Soc. **162**, A1265 (2015).

[31] N. Kyono, F. Bai, H. Nemori, H. Minami, D. Mori, Y. Takeda, O. Yamamoto, and N. Imanishi, Lithium-ion conducting solid electrolytes of $Li_{1.4}Al_{0.4}Ge_{0.2}Ti_{1.4}(PO_4)_3$ and MO_x (MâĂŕ=âĂŕAl, Ti, and Zr) composites, Solid State Ionics **324**, 114 (2018).

[32] F. Bai, K. Kakimoto, X. Shang, D. Mori, S. Taminato, M. Matsumoto, Y. Takeda, O. Yamamoto, H. Minami, H. Izumi, *et al.*, Synthesis of NASICON type $Li_{1.4}Al_{0.4}Ge_{0.2}Ti_{1.4}(PO_4)_3$ solid electrolyte by rheological phase method, J. Asian Ceram. Soc. **8**, 476 (2020).

[33] Y. Seino, T. Ota, K. Takada, A. Hayashi, and M. Tatsumisago, A sulphide lithium super ion conductor is superior to liquid ion conductors for use in rechargeable batteries, Energy Environ. Sci. **7**, 627 (2014).

[34] Z. Liu, W. Fu, E. A. Payzant, X. Yu, Z. Wu, N. J. Dudney, J. Kiggans, K. Hong, A. J. Rondinone, and C. Liang, Anomalous high ionic conductivity of nanoporous β-Li_3PS_4, J. Am. Chem. Soc. **135**, 975 (2013).

[35] B. R. Shin, Y. J. Nam, D. Y. Oh, D. H. Kim, J. W. Kim, and Y. S. Jung, Comparative study of TiS_2/Li-In all-solid-state lithium batteries using glass-ceramic Li_3PS_4 and $Li_{10}GeP_2S_{12}$ solid electrolytes, Electrochim. Acta **146**, 395 (2014).

[36] M. Takahashi, S. Yang, K. Yamamoto, K. Ohara, N. H. H. Phuc, T. Watanabe, T. Uchiyama, A. Sakuda, A. Hayashi,

M. Tatsumisago, *et al.*, Improvement of lithium ionic conductivity of Li_3PS_4 through suppression of crystallization using low-boiling-point solvent in liquid-phase synthesis, Solid State Ionics **361**, 115568 (2021).

[37] N. Kamaya, K. Homma, Y. Yamakawa, M. Hirayama, R. Kanno, M. Yonemura, T. Kamiyama, Y. Kato, S. Hama, K. Kawamoto, *et al.*, A lithium superionic conductor, Nat. Mater. **10**, 682 (2011).

[38] Y. Kato, K. Kawamoto, R. Kanno, and M. Hirayama, Discharge performance of all-solid-state battery using a lithium superionic conductor $Li_{10}GeP_2S_{12}$, Electrochemistry **80**, 749 (2012).

[39] J. Yin, X. Yao, G. Peng, J. Yang, Z. Huang, D. Liu, Y. Tao, and X. Xu, Influence of the Li–Ge–P–S based solid electrolytes on NCA electrochemical performances in all-solid-state lithium batteries, Solid State Ionics **274**, 8 (2015).

[40] Y. Li and J. Yu, Emerging applications of zeolites in catalysis, separation and host–guest assembly, Nat. Rev. Mater. **6**, 1156 (2021).

[41] C. Martinez and A. Corma, Inorganic molecular sieves: Preparation, modification and industrial application in catalytic processes, Coord. Chem. Rev. **255**, 1558 (2011).

[42] V. Van Speybroeck, K. Hemelsoet, L. Joos, M. Waroquier, R. G. Bell, and C. R. A. Catlow, Advances in theory and their application within the field of zeolite chemistry, Chem. Soc. Rev. **44**, 7044 (2015).

[43] Y. Li, L. Li, and J. Yu, Applications of zeolites in sustainable chemistry, Chem **3**, 928 (2017).

[44] Y. Li, X. Wang, J. Liang, K. Wu, L. Xu, and J. Wang, Design of a high performance zeolite/polyimide composite separator for lithium-ion batteries, Polymers **12**, 764 (2020).

[45] D. Chen, X. Wang, J. Liang, Z. Zhang, and W. Chen, A novel electrospinning polyacrylonitrile separator with dip-coating of zeolite and phenoxy resin for Li-ion batteries, Membranes **11**, 267 (2021).

[46] J. C. Barbosa, R. Gonçalves, C. M. Costa, V. de Zea Bermudez, A. Fidalgo-Marijuan, Q. Zhang, and S. Lanceros-Méndez, Materials advances as active fillers for lithium-ion battery solid polymer electrolytes, Mater. Adv. **2**, 3790 (2021).

[47] X. Chi, M. Li, J. Di, P. Bai, L. Song, X. Wang, F. Li, S. Liang, J. Xu, and J. Yu, A highly stable and flexible zeolite electrolyte solid-state Li–air battery, Nature **592**, 551 (2021).

[48] P. Hartmann, T. Leichtweiss, M. R. Busche, M. Schneider, M. Reich, J. Sann, P. Adelhelm, and J. Janek, Degradation of NASICON-type materials in contact with lithium metal: Formation of mixed conducting interphases (MCI) on solid electrolytes, J. Phys. Chem. C **117**, 21064 (2013).

[49] Y. Zhu, X. He, and Y. Mo, Origin of outstanding stability in the lithium solid electrolyte materials: Insights from thermodynamic analyses based on first-principles calculations, ACS Appl. Mater. Interfaces **7**, 23685 (2015).

[50] Y. Jin and P. J. McGinn, $Li_7La_3Zr_2O_{12}$ electrolyte stability in air and fabrication of a $Li/Li_7La_3Zr_2O_{12}/Cu_{0.1}V_2O_5$ solid-state battery, J. Power Sources **239**, 326 (2013).

[51] L. Cheng, E. J. Crumlin, W. Chen, R. Qiao, H. Hou, S. F. Lux, V. Zorba, R. Russo, R. Kostecki, Z. Liu, *et al.*, The origin of high electrolyte-electrode interfacial resistances in lithium cells containing garnet type solid electrolytes, Phys. Chem. Chem. Phys. **16**, 18294 (2014).

[52] F. Han, A. S. Westover, J. Yue, X. Fan, F. Wang, M. Chi, D. N. Leonard, N. J. Dudney, H. Wang, and C. Wang, High electronic conductivity as the origin of lithium dendrite formation within solid electrolytes, Nat. Energy **4**, 187 (2019).

[53] P. Birke, S. Scharner, R. A. Huggins, and W. Weppner, Electrolytic stability limit and rapid lithium insertion in the fast-ion-conducting $Li_{0.29}La_{0.57}TiO_3$ perovskite-type compound, J. Electrochem. Soc. **144**, L167 (1997).

[54] S. Wenzel, S. Randau, T. Leichtweiß, D. A. Weber, J. Sann, W. G. Zeier, and J. Janek, Direct observation of the interfacial instability of the fast ionic conductor $Li_{10}GeP_2S_{12}$ at the lithium metal anode, Chem. Mater. **28**, 2400 (2016).

[55] Y. S. Jung, D. Y. Oh, Y. J. Nam, and K. H. Park, Issues and challenges for bulk-type all-solid-state rechargeable lithium batteries using sulfide solid electrolytes, Isr. J. Chem. **55**, 472 (2015).

[56] G. Sahu, Z. Lin, J. Li, Z. Liu, N. Dudney, and C. Liang, Air-stable, high-conduction solid electrolytes of arsenic-substituted Li_4SnS_4, Energy Environ. Sci. **7**, 1053 (2014).

[57] A. Hayashi, H. Muramatsu, T. Ohtomo, S. Hama, and M. Tatsumisago, Improvement of chemical stability of Li_3PS_4 glass electrolytes by adding M_xO_y ($M = Fe$, Zn, and Bi) nanoparticles, J. Mater. Chem. A **1**, 6320 (2013).

[58] W. Xia, B. Xu, H. Duan, Y. Guo, H. Kang, H. Li, and H. Liu, Ionic conductivity and air stability of Al-doped $Li_7La_3Zr_2O_{12}$ sintered in alumina and Pt crucibles, ACS Appl. Mater. Interfaces **8**, 5335 (2016).

[59] C. Chen, Q. Wu, F. Chen, L. Zhang, S. Pan, C. Bian, X. Zheng, X. Meng, and F.-S. Xiao, Aluminium-rich beta zeolite-supported platinum nanoparticles for the low-temperature catalytic removal of toluene, J. Mater. Chem. A **3**, 5556 (2015).

[60] P. Bron, B. Roling, and S. Dehnen, Impedance characterization reveals mixed conducting interphases between sulfidic superionic conductors and lithium metal electrodes, J. Power Sources **352**, 127 (2017).

[61] A. Manthiram, X. Yu, and S. Wang, Lithium battery chemistries enabled by solid-state electrolytes, Nat. Rev. Mater. **2**, 16103 (2017).

[62] C. V. Amanchukwu, J. R. Harding, Y. Shao-Horn, and P. T. Hammond, Understanding the chemical stability of polymers for lithium−air batteries, Chem. Mater. **27**, 550 (2015).

[63] J. Dai, C. Yang, C. Wang, G. Pastel, and L. Hu, Interface engineering for garnet-based solid-state lithium-metal batteries: Materials, structures, and characterization, Adv. Mater. **30**, 1802068 (2018).

[64] P. Wang, W. Qu, W. L. Song, H. Chen, R. Chen, and D. Fang, Electro–chemo–mechanical issues at the interfaces in solid-state lithium metal batteries, Adv. Funct. Mater. **29**, 1900950 (2019).

[65] E. Shekarian, M. R. Jafari Nasr, T. Mohammadi, O. Bakhtiari, and M. Javanbakht, Preparation of 4A zeolite coated polypropylene membrane for lithium-ion batteries separator, J. Appl. Polym. Sci. **136**, 47841 (2019).

[66] C. Yu, Y. Li, M. Willans, Y. Zhao, K. R. Adair, F. Zhao, W. Li, S. Deng, J. Liang, M. N. Banis, *et al.*, Superionic conductivity in lithium argyrodite solid-state electrolyte by controlled Cl-doping, Nano Energy **69**, 104396 (2020).

[67] F. Sun, Y. Xiang, Q. Sun, G. Zhong, M. N. Banis, Y. Liu, R. Li, R. Fu, M. Zheng, T. K. Sham, *et al.*, Origin of high ionic conductivity of Sc-doped sodium-rich NASICON solid-state electrolytes, Adv. Funct. Mater. **31**, 2102129 (2021).

[68] Y. Wang, Y. Wu, Z. Wang, L. Chen, H. Li, and F. Wu, Doping strategy and mechanism for oxide and sulfide solid electrolytes with high ionic conductivity, J. Mater. Chem. A **10**, 4517 (2022).

[69] T. Famprikis, P. Canepa, J. A. Dawson, M. S. Islam, and C. Masquelier, Fundamentals of inorganic solid-state electrolytes for batteries, Nat. Mater. **18**, 1278 (2019).

[70] J. A. Dawson, P. Canepa, T. Famprikis, C. Masquelier, and M. S. Islam, Atomic-scale influence of grain boundaries on Li-ion conduction in solid electrolytes for all-solid-state batteries, J. Am. Chem. Soc. **140**, 362 (2018).

[71] N. C. Rosero-Navarro, T. Yamashita, A. Miura, M. Higuchi, and K. Tadanaga, Effect of sintering additives on relative density and Li-ion conductivity of Nb-doped $Li_7La_3ZrO_{12}$ solid electrolyte, J. Am. Ceram. Soc. **100**, 276 (2017).

[72] M. Hong, Q. Dong, H. Xie, B. C. Clifford, J. Qian, X. Wang, J. Luo, and L. Hu, Ultrafast sintering of solid-state electrolytes with volatile fillers, ACS Energy Lett. **6**, 3753 (2021).

[73] Z. Wang, Q. Ge, J. Shao, and Y. Yan, High performance zeolite LTA pervaporation membranes on ceramic hollow fibers by dipcoating–wiping seed deposition, J. Am. Chem. Soc. **131**, 6910 (2009).

[74] Q. Ge, Z. Wang, and Y. Yan, High-performance zeolite NaA membranes on polymer–zeolite composite hollow fiber supports, J. Am. Chem. Soc. **131**, 17056 (2009).

[75] Y. Ren, Y. Shen, Y. Lin, and C.-W. Nan, Direct observation of lithium dendrites inside garnet-type lithium-ion solid electrolyte, Electrochem. Commun. **57**, 27 (2015).

[76] M. Nagao, A. Hayashi, M. Tatsumisago, T. Kanetsuku, T. Tsuda, and S. Kuwabata, *In situ* SEM study of a lithium deposition and dissolution mechanism in a bulk-type solid-state cell with a Li_2S–P_2S_5 solid electrolyte, Phys. Chem. Chem. Phys. **15**, 18600 (2013).

[77] L. Porz, T. Swamy, B. W. Sheldon, D. Rettenwander, T. Fröemling, H. L. Thaman, S. Berendts, R. Uecker, W. C. Carter, and Y.-M. Chiang, Mechanism of lithium metal penetration through inorganic solid electrolytes, Adv. Energy Mater. **7**, 1701003 (2017).

[78] F. Mo, J. Ruan, S. Sun, Z. Lian, S. Yang, X. Yue, Y. Song, Y.-N. Zhou, F. Fang, G. Sun, *et al.*, Inside or outside: Origin of lithium dendrite formation of all solid-state electrolytes, Adv. Energy Mater. **9**, 1902123 (2019).

[79] F. Han, Y. Zhu, X. He, Y. Mo, and C. Wang, Electrochemical stability of $Li_{10}GeP_2S_{12}$ and $Li_7La_3Zr_2O_{12}$ solid electrolytes, Adv. Energy Mater. **6**, 1501590 (2016).

[80] Y.-T. Chen, A. Jena, W. K. Pang, V. K. Peterson, H.-S. Sheu, H. Chang, and R.-S. Liu, Voltammetric enhancement of Li-ion conduction in Al-doped $Li_{7-x}La_3Zr_2O_{12}$ solid electrolyte, J. Phys. Chem. C **121**, 15565 (2017).

[81] B. Xu, W. Li, H. Duan, H. Wang, Y. Guo, H. Li, and H. Liu, Li_3PO_4-added garnet-type $Li_{6.5}La_3Zr_{1.5}Ta_{0.5}O_{12}$ for Li-dendrite suppression, J. Power Sources **354**, 68 (2017).

[82] H.-S. Jeong, E.-S. Choi, S.-Y. Lee, and J. H. Kim, Evaporation-induced, close-packed silica nanoparticle-embedded nonwoven composite separator membranes for high-voltage/high-rate lithium-ion batteries: Advantageous effect of highly percolated, electrolyte-philic microporous architecture, J. Membr. Sci. **415–416**, 513 (2012).

[83] W. Na, K. H. Koh, A. S. Lee, S. Cho, B. Ok, S.-W. Hwang, J. H. Lee, and C. M. Koo, Binder-less chemical grafting of SiO_2 nanoparticles onto polyethylene separators for lithium-ion batteries, J. Membr. Sci. **573**, 621 (2019).

[84] J.-A. Choi, S. H. Kim, and D.-W. Kim, Enhancement of thermal stability and cycling performance in lithium-ion cells through the use of ceramic-coated separators, J. Power Sources **195**, 6192 (2010).

[85] Y. Lee, H. Lee, T. Lee, M.-H. Ryou, and Y. M. Lee, Synergistic thermal stabilization of ceramic/co-polyimide coated polypropylene separators for lithium-ion batteries, J. Power Sources **294**, 537 (2015).

[86] X. Jiang, X. Zhu, X. Ai, H. Yang, and Y. Cao, Novel ceramic-grafted separator with highly thermal stability for safe lithium-ion batteries, ACS Appl. Mater. Interfaces **9**, 25970 (2017).

[87] K. Peng, B. Wang, Y. Li, and C. Ji, Magnetron sputtering deposition of TiO_2 particles on polypropylene separators for lithium-ion batteries, RSC Adv. **5**, 81468 (2015).

[88] X. Zhu, X. Jiang, X. Ai, H. Yang, and Y. Cao, TiO_2 ceramic-grafted polyethylene separators for enhanced thermostability and electrochemical performance of lithium-ion batteries, J. Membr. Sci. **504**, 97 (2016).

[89] K. J. Kim, H. K. Kwon, M. S. Park, T. Yim, J. S. Yu, and Y. J. Kim, Ceramic composite separators coated with moisturized ZrO_2 nanoparticles for improving the electrochemical performance and thermal stability of lithium ion batteries, Phys. Chem. Chem. Phys. **16**, 9337 (2014).

[90] J. Nunes-Pereira, A. C. Lopes, C. M. Costa, L. C. Rodrigues, M. M. Silva, and S. Lanceros-Méndez, Microporous membranes of NaY zeolite/poly(vinylidene fluoride–trifluoroethylene) for Li-ion battery separators, J. Electroanal. Chem. **689**, 223 (2013).

[91] X. Dong, W. Mi, L. Yu, Y. Jin, and Y. S. Lin, Zeolite coated polypropylene separators with tunable surface properties for lithium-ion batteries, Microporous and Mesoporous Mater. **226**, 406 (2016).

[92] W. Xiao, Z. Gao, S. Wang, J. Liu, and C. Yan, A novel NaA-type zeolite-embedded composite separator for lithium-ion battery, Mater. Lett. **145**, 177 (2015).

[93] X. Mao, L. Shi, H. Zhang, Z. Wang, J. Zhu, Z. Qiu, Y. Zhao, M. Zhang, and S. Yuan, Polyethylene separator activated by hybrid coating improving Li^+ ion transference number and ionic conductivity for Li-metal battery, J. Power Sources **342**, 816 (2017).

[94] Z. Lu, H. Yang, Q.-H. Yang, P. He, and H. Zhou, Building a beyond concentrated electrolyte for high-voltage anode-free rechargeable sodium batteries, Angew. Chem. Int. Ed. **61**, e202200410 (2022).

[95] J. Xu, X. Xiao, S. Zeng, M. Cai, and M. W. Verbrugge, Multifunctional lithium-ion-exchanged zeolite-coated separator for lithium-ion batteries, ACS Appl. Energy Mater. **1**, 7237 (2018).

[96] Z. Chang, Y. Qiao, H. Yang, X. Cao, X. Zhu, P. He, and H. Zhou, Sustainable lithium-metal battery achieved by a safe electrolyte based on recyclable and low-cost molecular sieve, Angew. Chem. Int. Ed. **60**, 15572 (2021).

[97] H. Yang, Y. Qiao, Z. Chang, H. Deng, X. Zhu, R. Zhu, Z. Xiong, P. He, and H. Zhou, Reducing water activity by zeolite molecular sieve membrane for long-life rechargeable zinc battery, Adv. Mater. **33**, 2102415 (2021).

[98] X.-L. Wang, A. Mei, M. Li, Y.-H. Lin, and C.-W. Nan, Polymer composite electrolytes containing ionically active mesoporous SiO_2 particles, J. Appl. Phys. **102**, 054907 (2007).

[99] G. X. Wang, L. Yang, J. Z. Wang, H. K. Liu, and S. X. Dou, Enhancement of ionic conductivity of PEO based polymer electrolyte by the addition of nanosize ceramic powders, J. Nanosci. Nanotechnol. **5**, 1135 (2005).

[100] C. Ma, J. Zhang, M. Xu, Q. Xia, J. Liu, S. Zhao, L. Chen, A. Pan, D. G. Ivey, and W. Wei, Cross-linked branching nanohybrid polymer electrolyte with monodispersed TiO_2 nanoparticles for high performance lithium-ion batteries, J. Power Sources **317**, 103 (2016).

[101] S. Chen, Y. Zhao, J. Yang, L. Yao, and X. Xu, Hybrid solid electrolytes with excellent electrochemical properties and their applications in all-solid-state cells, Ionics **23**, 2603 (2017).

[102] Y. Huang, Z. Zhang, H. Gao, J. Huang, and C. Li, $Li_{1.5}Al_{0.5}Ti_{1.5}(PO_4)_3$ enhanced polyethylene oxide polymer electrolyte for all-solid-state lithium batteries, Solid State Ionics **356**, 115437 (2020).

[103] Y. Sun, X. Zhan, J. Hu, Y. Wang, S. Gao, Y. Shen, and Y. T. Cheng, Improving ionic conductivity with bimodal-sized $Li_7La_3Zr_2O_{12}$ fillers for composite polymer electrolytes, ACS Appl. Mater. Interfaces **11**, 12467 (2019).

[104] Y. Liu, B. Xu, W. Zhang, L. Li, Y. Lin, and C. Nan, Composition modulation and structure design of inorganic-in-polymer composite solid electrolytes for advanced lithium batteries, Small **16**, 1902813 (2020).

[105] M. Dirican, C. Yan, P. Zhu, and X. Zhang, Composite solid electrolytes for all-solid-state lithium batteries, Mater. Sci. Eng. R **136**, 27 (2019).

[106] J. Xi, X. Ma, M. Cui, X. Huang, Z. Zheng, and X. Tang, Electrochemistry study on PEO-$LiClO_4$-ZSM5 composite polymer electrolyte, Chin. Sci. Bull. **49**, 785 (2004).

[107] J. Xi, S. Miao, and X. Tang, Selective transporting of lithium ion by shape selective molecular sieves ZSM-5 in PEO-based composite polymer electrolyte, Macromolecules **37**, 8592 (2004).

[108] H. Jamal, F. Khan, S. Hyun, S. W. Min, and J. H. Kim, Enhancement of the ionic conductivity of a composite polymer electrolyte via surface functionalization of SSZ-13 zeolite for all-solid-state Li-metal batteries, J. Mater. Chem. A **9**, 4126 (2021).

[109] W. Li, S. Zhang, B. Wang, S. Gu, D. Xu, J. Wang, C. Chen, and Z. Wen, Nanoporous adsorption effect on alteration of the Li^+ diffusion pathway by a highly ordered porous electrolyte additive for high-rate all-solid-state lithium metal batteries, ACS Appl. Mater. Interfaces **10**, 23874 (2018).

[110] J. Xi, Y. Bai, X. Qiu, W. Zhu, L. Chen, and X. Tang, Conductivities and transport properties of microporous molecular sieves doped composite polymer electrolyte used for lithium polymer battery, New J. Chem. **29**, 1454 (2005).

[111] J. Xi, X. Qiu, M. Cui, X. Tang, W. Zhu, and L. Chen, Enhanced electrochemical properties of PEO-based composite polymer electrolyte with shape-selective molecular sieves, J. Power Sources **156**, 581 (2006).

[112] H. Jamal, F. Khan, H.-R. Si, and J. H. Kim, Enhanced compatibility of a polymer-based electrolyte with Li-metal for stable and dendrite-free all-solid-state Li-metal batteries, J. Mater. Chem. A **9**, 27304 (2021).

[113] G. Kelemen, W. Lortz, and G. Schön, Ionic conductivity of synthetic analcime, sodalite and offretite, J. Mater. Sci. **24**, 333 (1989).

[114] G. Kelemen and G. Schön, Ionic conductivity in dehydrated zeolites, J. Mater. Sci. **27**, 6036 (1992).

[115] P. Nischwitz, P. Amels, and F. Fetting, Studies on the ionic conductivity of zeolitic solids, Solid State Ionics **73**, 105 (1994).

[116] E. Jordan, R. G. Bell, D. Wilmer, and H. Koller, Anion-promoted cation motion and conduction in zeolites, J. Am. Chem. Soc. **128**, 558 (2006).

[117] O. Schäf, H. Ghobarkar, F. Adolf, and P. Knauth, Influence of ions and molecules on single crystal zeolite conductivity under *in situ* conditions, Solid State Ionics **143**, 433 (2001).

[118] U. Simon and U. Flesch, Cation-cation interaction in dehydrated zeolites X and Y monitored by modulus spectroscopy, J. Porous Mater. **6**, 33 (1999).

[119] M. Feuerstein and R. F. Lobo, Mobility of Li cations in X zeolites studied by solid-state NMR spectroscopy, Solid State Ionics **118**, 135 (1999).

[120] W. J. Mortier and R. A. Schoonheydt, Surface and solid state chemistry of zeolites, Prog. Solid St. Chem. **16**, 1 (1985).

[121] R. T. Pabalan and F. P. Bertetti, Cation-exchange properties of natural zeolites, Rev. Mineral. Geochem. **45**, 453 (2001).

[122] L. Wu and A. Navrotsky, Synthesis and thermodynamic study of transition metal ion (Mn^{2+}, Co^{2+}, Cu^{2+}, and Zn^{2+}) exchanged zeolites A and Y, Phys. Chem. Chem. Phys. **18**, 10116 (2016).

[123] N. Koike, K. Iyoki, B. Wang, Y. Yanaba, S. P. Elangovan, K. Itabashi, W. Chaikittisilp, and T. Okubo, Increasing the ion-exchange capacity of MFI zeolites by introducing Zn to aluminosilicate frameworks, Dalton Trans. **47**, 9546 (2018).

[124] H. Wang, X. Wang, M. Li, L. Zheng, D. Guan, X. Huang, J. Xu, and J. Yu, Porous materials applied in nonaqueous Li-O_2 batteries: Status and perspectives, Adv. Mater. **32**, 2002559 (2020).

[125] J. M. Shin, K. T. No, and M. S. Jhon, Molecular dynamics study on the Na ions bound in A-type zeolite framework, J. Phys. Chem. **92**, 4533 (1988).

[126] Y. Wang, W. D. Richards, S. P. Ong, L. J. Miara, J. C. Kim, Y. Mo, and G. Ceder, Design principles for

solid-state lithium superionic conductors, Nat. Mater. **14,** 1026 (2015).

[127] S. P. Culver, R. Koerver, T. Krauskopf, and W. G. Zeier, Designing ionic conductors: The interplay between structural phenomena and interfaces in thiophosphate-based solid-state batteries, Chem. Mater. **30,** 4179 (2018).

[128] K. Takada, Interfacial nanoarchitectonics for solid-state lithium batteries, Langmuir **29**, 7538 (2013).

[129] N. Ohta, K. Takada, L. Zhang, R. Ma, M. Osada, and T. Sasaki, Enhancement of the high-rate capability of solid-state lithium batteries by nanoscale interfacial modification, Adv. Mater. **18,** 2226 (2006).

[130] M. J. Lee, D. O. Shin, J. Y. Kim, J. Oh, S. H. Kang, J. Kim, K. M. Kim, Y. M. Lee, S. O. Kim, and Y.-G. Lee, Interfacial barrier free organic-inorganic hybrid electrolytes for solid state batteries, Energy Storage Mater. **37,** 306 (2021).

[131] H. Zhang, Y. Ren, X. Wu, and N. Wang, An interface-modified solid-state electrochemical device for lithium extraction from seawater, J. Power Sources **482,** 228938 (2021).

[132] Q. Liu, D. Zhou, D. Shanmukaraj, P. Li, F. Kang, B. Li, M. Armand, and G. Wang, Self-healing Janus interfaces for high-performance LAGP-based lithium metal batteries, ACS Energy Lett. **5,** 1456 (2020).

[133] F. Hu, Y. Li, Y. Wei, J. Yang, P. Hu, Z. Rao, X. Chen, L. Yuan, and Z. Li, Construct an ultrathin bismuth buffer for stable solid-state lithium metal batteries, ACS Appl. Mater. Interfaces **12,** 12793 (2020).

[134] J. Yu, Q. Liu, X. Hu, S. Wang, J. Wu, B. Liang, C. Han, F. Kang, and B. Li, Smart construction of multifunctional $Li_{1.5}Al_{0.5}Ge_{1.5}(PO_4)_3|Li$ intermediate interfaces for solid-state batteries, Energy Storage Mater. **46,** 68 (2022).

[135] S. Haber and M. Leskes, What can we learn from solid state NMR on the electrode–electrolyte Interface?, Adv. Mater. **30,** 1706496 (2018).

[136] P. Vadhva, J. Hu, M. J. Johnson, R. Stocker, M. Braglia, D. J. L. Brett, and A. J. E. Rettie, Electrochemical impedance spectroscopy for all-solid-state batteries: Theory, methods and future outlook, ChemElectroChem **8,** 1930 (2021).

[137] M. Severance, Y. Zheng, E. Heck, and P. K. Dutta, Influence of crystallite size on cation conductivity in faujasitic zeolites, J. Phys. Chem. A **117,** 13704 (2013).

[138] C. Zhang, Y. Feng, Z. Han, S. Gao, M. Wang, and P. Wang, Electrochemical and structural analysis in all-solid-state lithium batteries by analytical electron microscopy: Progress and perspectives, Adv. Mater. **32**, 1903747 (2020).

[139] X. Liu and L. Gu, Advanced transmission electron microscopy for electrode and solid-electrolyte materials in lithium-ion batteries, Small Methods **2,** 1800006 (2018).

[140] S. Shi, J. Gao, Y. Liu, Y. Zhao, Q. Wu, W. Ju, C. Ouyang, and R. Xiao, Multi-scale computation methods: Their applications in lithium-ion battery research and development, Chin. Phys. B **25,** 018212 (2016).

[141] X. Wu, Y. Dou, R. Lian, Y. Wang, and Y. Wei, Understanding rechargeable magnesium ion batteries via first-principles computations: A comprehensive review, Energy Storage Mater. **48,** 344 (2022).

[142] Y. Sun, T. Yang, H. Ji, J. Zhou, Z. Wang, T. Qian, and C. Yan, Boosting the optimization of lithium metal batteries by molecular dynamics simulations: A perspective, Adv. Energy Mater. **10,** 2002373 (2020).

[143] M. Yang, Y. Liu, A. M. Nolan, and Y. Mo, Interfacial atomistic mechanisms of lithium metal stripping and plating in solid-state batteries, Adv. Mater. **33,** 2008081 (2021).

[144] N. Yao, X. Chen, Z. H. Fu, and Q. Zhang, Applying classical, *ab initio*, and machine-learning molecular dynamics simulations to the liquid electrolyte for rechargeable batteries, Chem. Rev. **122,** 10970 (2022).

[145] A. M. Nolan, Y. Zhu, X. He, Q. Bai, and Y. Mo, Computation-accelerated design of materials and interfaces for all-solid-state lithium-ion batteries, Joule **2,** 2016 (2018).

[146] Y. Li, K. Leung, and Y. Qi, Computational exploration of the Li-electrode|electrolyte interface in the presence of a nanometer thick solid-electrolyte interphase layer, Acc. Chem. Res. **49,** 2363 (2016).

[147] T. C. T. Pham, T. H. Nguyen, and K. B. Yoon, Gel-free secondary growth of uniformly oriented silica MFI zeolite films and application for xylene separation, Angew. Chem. Int. Ed. **52,** 8693 (2013).

[148] S. Pan, X. Meng, Z. Wang, Y. Yan, and F.-S. Xiao, An efficient synthesis of NaA zeolite membranes from direct crystallization of gel-dipped macroporous alumina tubes with seeds, J. Mater. Chem. A **6,** 10484 (2018).

[149] Y. Huang, L. Wang, Z. Song, S. Li, and M. Yu, Growth of high-quality, thickness-reduced zeolite membranes towards N_2/CH_4 separation using high-aspect-ratio seeds, Angew. Chem. Int. Ed. **54,** 10843 (2015).

[150] N. Chang, H. Tang, L. Bai, Y. Zhang, and G. Zeng, Optimized rapid thermal processing for the template removal of SAPO-34 zeolite membranes, J. Membr. Sci. **552,** 13 (2018).

[151] C. Zhou, C. Yuan, Y. Zhu, J. Caro, and A. Huang, Facile synthesis of zeolite FAU molecular sieve membranes on bio-adhesive polydopamine modified Al_2O_3 tubes, J. Membr. Sci. **494,** 174 (2015).

[152] H. Dou, M. Xu, B. Wang, Z. Zhang, G. Wen, Y. Zheng, D. Luo, L. Zhao, A. Yu, L. Zhang, *et al.*, Microporous framework membranes for precise molecule/ion separations, Chem. Soc. Rev. **50,** 986 (2021).

[153] H. Kitaura and H. Zhou, Electrochemical performance of solid-state lithium–air batteries using carbon nanotube catalyst in the air electrode, Adv. Energy Mater. **2,** 889 (2012).

[154] Y. Liu, B. Li, H. Kitaura, X. Zhang, M. Han, P. He, and H. Zhou, Fabrication and performance of all-solid-state Li–air battery with SWCNTs/LAGP cathode, ACS Appl. Mater. Interfaces **7,** 17307 (2015).

[155] J. Sun, N. Zhao, Y. Li, X. Guo, X. Feng, X. Liu, Z. Liu, G. Cui, H. Zheng, L. Gu, *et al.*, A rechargeable Li-air fuel cell battery based on garnet solid electrolytes, Sci. Rep. **7,** 41217 (2017).